# Beyond Boundaries: A Novel Data-Augmentation Discourse for Open Domain Generalization

**Anonymous authors**
**Paper under double-blind review**

## Abstract

The problem of Open Domain Generalization (ODG) is multifaceted, encompassing shifts in domains and labels across all source and target domains. Existing approaches have encountered challenges such as style bias towards training domains, insufficient feature-space disentanglement to highlight semantic features, and discriminativeness of the latent space. Additionally, they rely on a confidence-based target outlier detection approach, which can lead to misclassifications when target open samples visually align with the source domain data. In response to these challenges, we present a solution named ODG-NET. We aim to create a direct open-set classifier within a *discriminative*, *unbiased*, and *disentangled* semantic embedding space. To enrich data density and diversity, we introduce a generative augmentation framework that produces *style-interpolated* novel domains for closed-set images and novel pseudo-open images by *interpolating the contents of paired training images*. Our augmentation strategy skillfully utilizes *disentangled style and content information* to synthesize images effectively. Furthermore, we tackle the issue of style bias by representing all images in relation to all source domain properties, which effectively accentuates complementary visual features. Consequently, we train a multi-class semantic object classifier, incorporating both closed and open class classification capabilities, along with a style classifier to identify style primitives. The joint use of style and semantic classifiers facilitates the disentanglement of the latent space, thereby enhancing the generalization performance of the semantic classifier. To ensure discriminativeness in both closed and open spaces, we optimize the semantic feature space using novel metric losses. The experimental results on six benchmark datasets convincingly demonstrate that ODG-NET surpasses the state-of-the-art by an impressive margin of $1 - 4\%$ in both open and closed-set DG scenarios.

## 1 Introduction

Domain Generalization (DG) Zhou et al. (2022) aims to create a shared embedding space from labeled *source* domains, applicable to an unseen *target* domain. However, existing DG techniques primarily operate in a closed-set setting Zhou et al. (2020b;a), where the source and target domains share the same label spaces. Unfortunately, this approach may not always be practical in dynamic real-world scenarios, such as Robotics, where a robot navigating its environment may encounter both shared and environment-specific categories Zhao & Shen (2022). This realization highlights the need to address the more realistic and challenging scenario of Open Domain Generalization (ODG) Shu et al. (2021), involving training on labeled source domains with both shared and domain-specific categories. The target domain, in this case, comprises samples from either known classes or novel classes exclusive to the target domain, presenting several significant challenges. Firstly, severe data imbalance arises due to the unequal representation of known classes in the source domains. Secondly, achieving a domain-agnostic and discriminative embedding space becomes challenging due to unrestricted domain and label shifts. Thirdly, there is a lack of prior knowledge about the open space in the target domain. While one naive solution to ODG could involve combining an existing closed-set DG technique with an off-the-shelf open-set recognition (OSR) approach like Openmax Bendale & Boult (2016b), this approach may prove sub-optimal. The DG technique is likely to be influenced by the domain-specific classes present in ODG, which suffer from severe under-representation.

Remarkably, ODG techniques have yet to garner significant attention in the DG literature, leaving DAML Shu et al. (2021) as the solitary model explicitly tailored for ODG. Nevertheless, our thorough investigation has uncovered

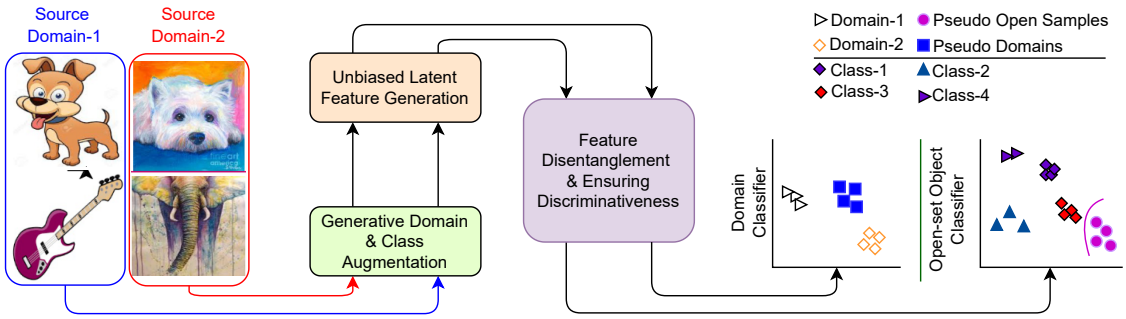


Figure 1: The working principle of ODG-NET. Given a number of source domains with shared and private classes for each domain, our algorithm follows three simple stages to obtain an effective semantic open-set object classifier, as depicted in the figure.

three potential limitations of DAML. Firstly, DAML augments the available source domains with multi-domain mix-up features, utilizing a Dirichlet-distribution based weighting scheme where the same weight configuration signifies the label for the generated feature. The fusion of content and style information in the raw latent features could potentially lead to semantically incoherent feature and label pairs. Our validation through a straightforward multi-label classification experiment on the PACS dataset Li et al. (2017) demonstrated notably poor accuracy for classifying the synthesized features. Secondly, DAML overlooks the vital aspect of disentangling content features from domain properties. As a result, the model may exhibit biases towards certain styles, impeding its adaptability to diverse visual domains. Thirdly, DAML's outlier rejection strategy relies on thresholding the responses of an ensemble of source domain classifiers. This approach may yield erroneous outcomes, particularly when target open samples exhibit visual coherence with some of the source domain classes. These limitations highlight the need for further exploration and refinement of ODG techniques to unleash their full potential and address the complexities meaningfully.

In our quest to overcome the aforementioned limitations, we present a novel approach for training a powerful generalized semantic open-set classifier, endowed with the unique ability to discern both closed-set and potential open samples within an *unbiased* and *disentangled* embedding space. However, accomplishing this requires representative open-space samples for training the classifier, which, regrettably, are not available during the training phase. To overcome this hurdle, we propose sample hallucination, ingeniously crafting a way to generate these essential samples to facilitate the comprehensive training of our classifier. Furthermore, we acknowledge and address the challenge of class imbalance in ODG. Our strategy involves augmenting the diversity in appearance of the training classes. As we progress, we diligently focus on representing the images in a feature space that remains unswayed by the nuances of the training domains. To this end, we propose segregating the semantic features from the style primitives, unlocking the true essence of each image's content. Finally, our journey culminates in ensuring that the semantic space is inherently class-discriminative, allowing our classifier to make decisive and accurate distinctions between various categories.

**Our proposed ODG-NET**: In this paper, we propose ODG-NET (Fig. 1), a discriminative model to address the concerns raised above. Our model comprises three crucial modules, each dedicated to tackle the model bias, feature disentanglement, and discriminative semantic feature space learning, respectively.

At the core of our research lies the objective to augment the available source domains through two distinct types of synthesized images from a novel conditional GAN, each serving specific goals: the enrichment of closed-set class diversities and the generation of representative pseudo-open images. The first type, aptly named domain or style mix-up images, involves a sophisticated interpolation of the style properties from the source domains using a Dirichlet distribution. This approach gives rise to novel domains that diversify the style of the source images while meticulously preserving their intrinsic semantic object properties. The second type, known as pseudo open-space images, emerges through a skillful interpolation of both domain and class identifiers from the source domain images using Dirichlet sampling. To ensure the creation of diverse and meaningful samples, we have introduced a diversification regularization to safeguard against potential mode collapse during the generation of domain or label-interpolated samples. Additionally, we have implemented a structural cycle consistency mechanism, thereby upholding the structural superiority of the generated images. Our approach takes on several formidable challenges, ranging from class imbalance and

limited style diversity to the absence of an open-space prior. A distinguishing feature of our methodology lies in its ability to unify the concepts of label and domain mix-up while granting the flexibility to tailor individual conditioning. In this manner, we transcend existing augmentation methods, which merely perform style or random image mix-ups Mancini et al. (2020a); Zhou et al. (2021).

Our model aims for an unbiased latent embedding space, free from source domain bias. We achieve this through a novel approach of training domain-specific classifiers, expertly capturing domain-specific features from each source domain. Each image is then represented as a concatenation of features from all domain-specific models, creating a comprehensive and unbiased embedding.

We strive to disentangle domain-specific properties from semantic object features within the latent representations. To this end, we train two attention-driven classifiers: a domain classifier identifying the domain label and an object classifier recognizing class labels from the augmented domain set, enriching our model's understanding of object semantics, while reducing the effects of the domain-specific artifacts considerably.

Ensuring a highly discriminative semantic feature space, we introduce a contrastive loss among known classes, sharpening the distinction between different categories. Moreover, our entropy minimization objective strategically pushes pseudo outliers far from the known-class boundary, enhancing the model's robustness.

We summarize our **major contributions** as:

[-] In this paper, we present ODG-NET, an end-to-end network that tackles the challenging ODG problem by jointly considering closed and open space domain augmentation, feature disentanglement, and semantic feature-space optimization.

[-] To synthesize augmented images that are diverse from the source domains, we propose a novel conditional GAN with a cycle consistency constraint and an anti-mode-collapse regularizer that interpolates domain and category labels. We also adopt a classification-based approach for feature disentanglement. Finally, we ensure the separability of the semantic feature space for closed and open classes through novel metric objectives.

[-] We evaluate ODG-NET on six benchmark datasets in both open and closed DG settings. Our experiments demonstrate that ODG-NET consistently outperforms the literature. For instance, on ODG for Multi-dataset Shu et al. (2021) and on closed DG for DomainNet Peng et al. (2019), ODG-NET outperforms the previous state-of-the-art by approximately $3\%$.

## 2 Related Works

**(Open) DG**. The initial studies in closed-set DG focused on domain adaptation (DA) Li et al. (2020); Wang et al. (2021); Li et al. (2021a) due to the disparity in domain distributions. Several DG methods have since been developed, such as self-supervised learning Carlucci et al. (2019), ensemble learning Xu et al. (2014), and meta-learning Patricia & Caputo (2014); Wang et al. (2020b); Li et al. (2019b; 2018a; 2019a); Huang et al. (2020). To address the domain disparity, the concept of domain augmentation Li et al. (2021c); Kang et al. (2022); Zhou et al. (2020b; 2021); Zhang et al. (2022) was introduced, which involves generating pseudo-domains and adding them to the available pool of domains. Subsequently, the notion of ODG was introduced in Shu et al. (2021), which is based on domain-augmented meta-learning. To solve the single-source ODG problem, Zhu & Li (2021) and Yang et al. (2022) further extended the idea of multi-source ODG. See Zhou et al. (2022) for more discussions on DG.

*Our proposed* ODG-NET *represents a significant departure from DAML Shu et al. (2021). Unlike their ad-hoc feature-level mix-up strategy, we introduce a more robust augmentation technique that leverages generative modeling to seamlessly synthesize pseudo-open and closed set image samples. Additionally, we take a direct approach to learning an open-set classifier in a meaningful and optimized semantic space, in contrast to the source classifier's confidence-driven inference used in Shu et al. (2021). As a result,* ODG-NET *is better suited to handling open samples of different granularities.*

**Augmentation in DG**. Data augmentation is a crucial technique in DG, and it can be implemented using various methods such as variational autoencoders, GANs, and mixing strategies Goodfellow et al. (2020); Kingma & Welling (2013); Zhang et al. (2017). For instance, Rehman *et al.* Rahman et al. (2019) used ComboGAN to generate new data and optimized ad hoc domain divergence measures to learn a domain-generic space. Zhou *et al.* Zhou et al. (2020b)

combined GAN-based image generation with optimal transport to synthesize images different from the source data. Gong *et al.* Gong et al. (2019) treated generation as an image-to-image translation process and extracted intermediate images given an image pair. Similarly, Li et al. (2021b) used adversarial training to generate domains instead of samples. Mix-up, on the other hand, generates new data by interpolating between a pair of samples and their labels. Recently, mix-up techniques Yun et al. (2019); Mancini et al. (2020a); Zhou et al. (2021) have become popular in the DG literature, applied to either the image or feature space.

The augmentation approach used by ODG-NET stands out from the existing literature by going beyond simple style or image mix-up. Our approach ensures that the object properties of images remain intact when using style mix-up, and we also have control over label mix-up to generate pseudo-open samples that can scatter the open space with varying levels of similarity to the source domains.

*Among the existing augmentation strategies, Zhou et al. (2020b) and Gong et al. (2019) are the closest to our approach as they both use conditional GANs. However, there are several key differences between our method and theirs: (a) Gong et al. (2019) requires paired training data to sample intermediate pseudo-stylized images, whereas we use conditional generation without the need for paired data; (b) Zhou et al. (2020b) uses extrapolation for domains, which is ill-posed, while we use Dirichlet distributions to interpolate domains and classes; and (c) while both Zhou et al. (2020b) and Gong et al. (2019) use style mix-up for closed-set data, we generate both closed and pseudo-open samples judiciously.*

**Disentangled representation learning**. Disentangled feature learning refers to the process of modeling distinct and explanatory data variation factors. As per Dittadi et al. (2020), disentanglement can aid in out-of-distribution tasks. Previous efforts have focused on disentangling semantic and style latent variables in the original feature space using encoder-decoder models Wang et al. (2022); Cai et al. (2019), causality Ouyang et al. (2021), or in the Fourier space Wang et al. (2022). These models are complex and require sophisticated knowledge to improvement the feature learning of the models. *In contrast,* ODG-NET *proposes to use simple to implement yet effective, attention-based classifiers, to separate the style and semantic primitives from the latent visual representations.*

## 3 Problem Definition and Proposed Methodology

In the context of ODG, we have access to multiple source domains denoted as $\mathcal{D} = \{\mathcal{D}_1, \mathcal{D}_2, \cdots, \mathcal{D}_{\mathcal{S}}\}$. Each of these domains has different distributions and contains a combination of domain-specific and shared categories. During training, we use labeled samples from each domain $\mathcal{D}_s = (x_s^i, y_s^i)_{i=1}^{n_s}$, where $y_s \in \mathcal{Y}_s$ is the label for $x_s \in \mathcal{X}_s$. The total number of classes in $\mathcal{D}$ is denoted by $\mathcal{C}$. The target domain $\mathcal{D}_{\mathcal{T}} = \{x_t^j\}_{j=1}^{n_t}$ has a distribution that is different from that of $\mathcal{D}$. It consists of unlabeled samples that belong to one of the source classes present in $\mathcal{D}$ or novel classes that were not seen during training. The objective is to model a common classifier that can reject outliers while properly recognizing the known class samples given $\mathcal{D}$ and then evaluate its performance on $\mathcal{D}_{\mathcal{T}}$.

In our formulation, each domain/style in $\mathcal{D}$ is represented using an $\mathcal{S}$-dimensional one-hot vector $v_d$. In contrast, a pseudo-domain (synthesized style) is represented by $\hat{v}_d$, which is sampled from a Dirichlet distribution with parameter $\alpha$ and has the same length as $v_d$. For instance, if $\mathcal{S} = 3$, a source domain can be represented as a three-dimensional one-hot vector (e.g., $[0, 0, 1]$), while a $\hat{v}_d$ could be $[0.2, 0.3, 0.5]$.

Similarly, we denote the label $y$ as a $\mathcal{C}$-dimensional one-hot vector. On the other hand, an interpolated label space is represented by $\hat{y}$, which is sampled in the same way as $\hat{v}_d$. A real image-label pair from $\mathcal{D}$ is denoted as $(x_r, y)$. In contrast, a cGAN synthesized image is denoted by $(x_f^{cs}, y)$ or $(x_f^{os}, \hat{y})$ depending on whether it represents a style-interpolated closed-set image with label $y$ or a joint style and label interpolated pseudo-open image with label $\hat{y}$, respectively. Finally, to aid in open-set classification, we introduce a label space $\tilde{y} \in \mathbb{R}^{\mathcal{C}+1}$. The first $\mathcal{C}$ indices are reserved for closed-class samples, while the $\mathcal{C}+1$-th index is used for pseudo-outlier samples.

### 3.1 Model and training overview for ODG-NET

We aim to design a direct open-set classifier that operates in a disentangled, discriminative, and unbiased semantic feature space. To achieve our goals, we introduce ODG-NET, which consists of four modules (see Fig. 2). Firstly, ODG-NET employs a generative augmentation strategy, using a **conditional GAN** equipped with a U-Net based generator $\mathcal{F}_G$ and a binary discriminator $\mathcal{F}_{disc}$. We condition $\mathcal{F}_G$ on four variables: domain label $v_d/\hat{v}_d$, class label

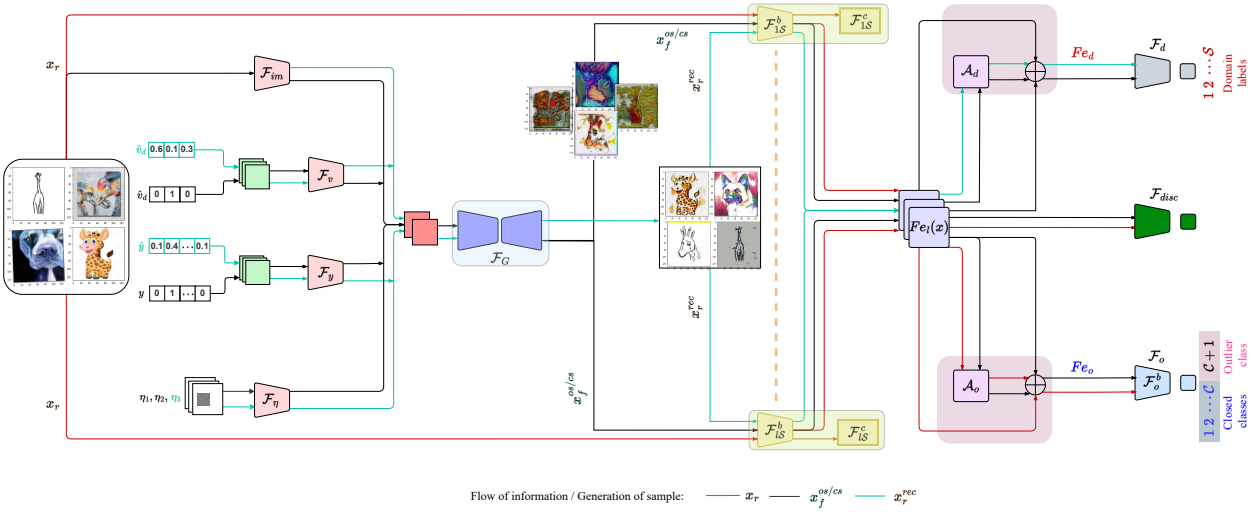


Figure 2: A depiction of the ODG-NET architecture. It shows the model components: the embedding networks: $(\mathcal{F}_{im}, \mathcal{F}_v, \mathcal{F}_y, \mathcal{F}_\eta)$, cGAN consisting of $(\mathcal{F}_G, \mathcal{F}_{disc})$, the local domain-specific classifiers $\{\mathcal{F}_l^s = (\mathcal{F}_{ls}^b, \mathcal{F}_{ls}^c)\}_{s=1}^{\mathcal{S}}$, and the global domain and semantic classifiers $(\mathcal{F}_d, \mathcal{F}_o)$ with corresponding attention blocks $\mathcal{A}_d$ and $\mathcal{A}_o$, respectively. Colors indicate the flow of information for different data items.

$y/\hat{y}$, an input image $x_r/x_f^{cs}/x_f^{os}$, and noise tensor $\eta_1/\eta_2/\eta_3$ sampled from predefined distributions. To ensure that the conditioning variables are combined correctly, we propose using separate embedding networks $(\mathcal{F}_{im}, \mathcal{F}_v, \mathcal{F}_y, \mathcal{F}_\eta)$ to encode the image, domain label, class label, and noise into meaningful latent representations. We train $\mathcal{F}_G$ to generate two types of images: (i) $(x_f^{cs}, y)$ when conditioned on $(x_r, \hat{v}_d, y, \eta_1)$, where $x_f^{cs}$ preserves the class label $y$ of $x_r$ while the style changes according to $\hat{v}_d$, and (ii) $(x_f^{os}, \hat{y})$ when conditioned on $(x_r, v_d/\hat{v}_d, \hat{y}, \eta_2)$, which changes the semantic and style information of $x_r$ according to $\hat{y}$ and $v_d/\hat{v}_d$ in $x_f^{os}$. We use a standard min-max formulation to train the cGAN and introduce a regularizer to prevent the generated samples from residing in a closer vicinity with the data from $\mathcal{D}$ (Eq. 1). A cycle consistency loss is further introduced to maintain the semantic regularity of the generated images (Eq. 2).

To obtain an unbiased latent feature space, we propose to represent all the images with respect to the feature space of all source domains. We introduce $\mathcal{S}$ **local source-domain specific networks** consisting of a feature backbone and a classification module, e.g., $\mathcal{F}_l^s = (\mathcal{F}_{ls}^b, \mathcal{F}_{ls}^c)$, which is trained on $\mathcal{D}_s$. We combine feature responses from all $\mathcal{F}_{ls}^b$ to obtain the latent representation $Fe_l(x) = [\mathcal{F}_{l1}^b; \mathcal{F}_{l2}^b; \cdots; \mathcal{F}_{l\mathcal{S}}^b]$ for a given image $x$ (Eq. 3).

To disentangle domain-dependent properties from semantic object features from $Fe_l(x)$, we introduce **global domain and semantic object classifiers** denoted by $\mathcal{F}_d$ with $\mathcal{S}$ output nodes and $\mathcal{F}_o$ with $\mathcal{C}+1$ output nodes (Eq. 4-5), shared across domains. We use spectral-spatial self-attention modules $\mathcal{A}_d$ and $\mathcal{A}_o$ to highlight domain and semantic object features from $Fe_l$, denoted by $Fe_d$ and $Fe_o$, and seek to ensure discriminativeness of the semantic embedding space (outputs of the feature encoder of $\mathcal{F}_o$, denoted by $\mathcal{F}_o^b$) through novel metric losses, encouraging the separation of all closed and pseudo-open class samples (Eq. 6-7). In the following, we discuss the proposed loss functions.

### 3.2 Loss functions, training, and inference

**Regularized cGAN objectives with structural cycle consistency**. To generate synthetic images, $\mathcal{F}_G$ and $\mathcal{F}_{disc}$ engage in a min-max adversarial game. The goal of $\mathcal{F}_{disc}$ is to accurately identify the real/fake domains of the images, while $\mathcal{F}_G$ aims to trick $\mathcal{F}_{disc}$. Hence, in order to ensure that the generated images are not collapsed with $\mathcal{D}$, for a given pair of real and synthesized image features $Fe_l(x_r)$ and $Fe_l(x_f^{cs/os})$, we propose a regularizer $\mathcal{W}$ that penalizes the situation if $x_r$ and $x_f^{cs/os}$ are identical for slightly different $(v_d, \hat{v}_d)$ or $(y_d, \hat{y}_d)$. $\delta$ is the `cosine` similarity and $\epsilon$ is a small constant. Crisply, even if $\delta(v_d, \hat{v}_d)$ or $\delta(y_d, \hat{y}_d) \to 1$, $\mathcal{W}$ will enforce $\delta(Fe_l(x_r), Fe_l(x_f^{cs/os})) \to 0$ to minimize the loss. The total loss is mentioned below.

$$\mathbf{L_{Gan}} = \mathop{\mathbb{E}}_{P_{\mathcal{D}}, P_{noise}^{os/cs}}[log(\mathcal{F}_{disc}(Fe_l(x_r))) + log(1 - \mathcal{F}_{disc}(Fe_l(x_f^{cs/os}))) + \beta \underbrace{\frac{\delta(Fe_l(x_r), Fe_l(x_f^{os/cs})) + \epsilon}{\delta(v_d, \hat{v}_d) + \delta(y_d, \hat{y}_d) + \epsilon}}_{\mathcal{W}}]. \tag{1}$$

In this context, $P_{\mathcal{D}}$, $P_{noise}^{cs}$, and $P_{noise}^{os}$ denote the data distribution of the source domains in $\mathcal{D}$ and the noise used to generate closed-set and open-set samples, respectively. We set $P_{noise}^{cs} = \mathcal{N}(0, \mathbb{I})$, and $P_{noise}^{os} = \mathcal{N}(0, \sigma)$, where $\sigma$ is a large value. Our goal is to limit the space of generated closed-set images so that they represent similar semantic concepts while allowing for more scattering in the pseudo-open space, aiding in learning a robust open-set classifier.

To maintain the structural robustness of $\mathcal{F}_G$ against variations in style or label, we propose a method for reconstructing $x_r$. We take into account the embeddings of the synthesized $x_f^{cs/os}$, the actual class label $y$, the domain identifier $v_d$, and a noise vector $\eta_3 \in \mathcal{N}(0, \mathbb{I})$ as inputs to $\mathcal{F}_G$: $x_r^{rec} = \mathcal{F}_G(x_f^{os/cs}, v_d, y, \eta_3)$. By following the path $x_r \rightarrow x_f^{cs/os} \rightarrow x_r^{rec}$, we ensure that $x_f^{cs/os}$ represents a meaningful image rather than noisy data.

To compute the loss, we use the standard $\ell_1$ distance between the original real domain images and the remapped images $x_r^{rec}$, given by:

$$\mathbf{L_{rec}} = \mathop{\mathbb{E}}_{P_{\mathcal{D}}, \mathcal{N}(0,\mathbb{I})} [||x_r - x_r^{rec}||_1^1]. \tag{2}$$

**Learning style agnostic latent representations**. To prevent the model from overfitting to any particular source domain, we propose a method where input images are represented based on the properties of all source domains using $Fe_l(x)$. This creates a multiview representation space that captures complementary perspectives of the images.

To achieve this, we train $\mathcal{F}_l^s$ using $\mathcal{D}_s$ where $s$ belongs to $\{1, 2, \cdots, \mathcal{S}\}$. We consider $\mathcal{S}$ multiclass cross-entropy losses ($\mathbf{L_{CE}}$) for this purpose (as shown in Eq. 3), where $P_{\mathcal{D}}^s$ represents the data distribution for the $s^{th}$ source domain.

$$\mathbf{L_{local}} = \frac{1}{\mathcal{S}} \sum_{s \in \{1,2,\cdots,\mathcal{S}\}} \mathop{\mathbb{E}}_{P_{\mathcal{D}}^s} [\mathbf{L_{CE}}(\mathcal{F}_{ls}^c(x_s), y_s)]. \tag{3}$$

**Disentangling latent features through global classifiers**. The global domain classifier, $\mathcal{F}_d$, aims to identify the domain identifiers based on the attended features, $Fe_d(x) = Fe_l(x) \otimes \mathcal{A}_d + Fe_l(x)$, using a multiclass cross-entropy loss. We observe that $\mathcal{F}_d$ implicitly ensures that $\mathcal{F}_G$ generates images according to the conditioning domain identifiers. The corresponding loss function is presented below.

$$\mathbf{L_{dom}} = \mathop{\mathbb{E}}_{P_{\mathcal{D}}, P_{noise}^{cs/os}} [\mathbf{L_{CE}}(\mathcal{F}_d(\underbrace{Fe_d(x_r^{rec})}_{\text{domain features}}), v_d) + \mathbf{L_{CE}}(\mathcal{F}_d(\underbrace{Fe_d(x_f^{os/cs})}_{\text{domain features}}), \hat{v}_d)]. \tag{4}$$

In contrast, the open-set classifier, $\mathcal{F}_o$, is trained to accurately identify all samples belonging to known classes while disregarding the generated pseudo-outliers by labeling them as $\mathcal{C} + 1$, from $Fe_o(x) = Fe_l(x) \otimes \mathcal{A}_o + Fe_l(x)$. This is achieved using a multiclass cross-entropy loss. Similar to $\mathcal{F}_d$, $\mathcal{F}_o$ also aids $\mathcal{F}_G$ in producing high-quality synthesized images and supplements $\mathbf{L_{rec}}$.

$$\mathbf{L_{class}} = \mathop{\mathbb{E}}_{P_{\mathcal{D}}, P_{noise}^{cs/os}} [\mathbf{L_{CE}}(\mathcal{F}_o(\underbrace{Fe_o(x_r)}_{\text{object features}}), \tilde{y}) + \mathbf{L_{CE}}(\mathcal{F}_o(\underbrace{Fe_o(x_f^{cs/os})}_{\text{object features}}), \tilde{y})]. \tag{5}$$

$\mathcal{F}_d$ and $\mathcal{F}_o$ work together on $Fe_l(x)$, and seek to learn the domain-specific and semantic features separately, suggesting that fact that both the networks are devoted to disentangling the latent features wisely.

**Ensuring discriminativeness of the semantic feature space**. The inherent variations in multi-domain data make it challenging for $\mathcal{F}_o$ to generate an optimized semantic feature space from $\mathcal{F}_o^b$, where closed-set classes over the augmented domains are expected to form distinct groups, and pseudo-open-set samples, are deemed to be pushed away from the support of the closed set. To promote discriminativeness, we suggest using a contrastive loss for closed-set samples across the augmented domain set while also minimizing the entropy ($\mathcal{E}$) of $\mathcal{F}_o$ predictions for pseudo-open samples. This, in turn, acts as a weighting to $\mathcal{F}_o$ for the pseudo-open samples, which increases $p(y = \mathcal{C} + 1 | x_f^{cs/os})$ while reducing the posteriors for the known-class indices $(1 - \mathcal{C})$.

To implement the contrastive loss, $\mathbf{L_{con}}$, we select an anchor sample, $x_a$, and randomly obtain a positive sample, $x_+$, which shares the same class label as $x_a$, as well as a set of negative samples, $\{x_-^m\}_{m=1}^M$, where no restrictions are imposed on the styles of the samples. The goal is to maximize the cosine similarity, $\delta$, for $(x_a, x_+)$, while minimizing it for all possible pairs of $(x_a, x_-^m)$. The semantic feature space optimization loss can be expressed as follows:

$$\mathbf{L_{sem}} = \mathop{\mathbb{E}}_{P_{\mathcal{D}}, P_{noise}^{os/cs}} [\mathcal{E}(\mathcal{F}_o(Fe_o(x_f^{os}))) + \mathbf{L_{con}}]. \tag{6}$$

where $\mathbf{L_{con}}$ is defined as follows,

$$\mathbf{L_{con}} = [-\log \frac{\exp(\delta(\mathcal{F}_o^b(x_a), \mathcal{F}_o^b(x_+))}{\sum_{m=1}^M \exp(\delta(\mathcal{F}_o^b(x_a), \mathcal{F}_o^b(x_-^m))}]. \tag{7}$$

**Total loss and training**. We follow an alternate optimization strategy in each training episode for ODG-NET, mentioned in Algorithm 1. In the vanilla training stage, we train the embedding networks $(\mathcal{F}_{im}, \mathcal{F}_v, \mathcal{F}_y, \mathcal{F}_\eta)$, GAN modules $\mathcal{F}_G$, $\mathcal{F}_{disc}$, and the local domain-specific networks $\{\mathcal{F}_l^s\}_{s=1}^{\mathcal{S}}$, given the fixed $(\mathcal{F}_d, \mathcal{F}_o)$ to produce meaningful images. $w$s represent the loss contributions and *we set them to the value* 1 *in all our experiments*.

$$\mathop{\text{argmin}}_{\substack{\mathcal{F}_{im}, \mathcal{F}_v, \mathcal{F}_y, \mathcal{F}_\eta, \mathcal{F}_G, \\ \{\mathcal{F}_l^s\}_{s=1}^{\mathcal{S}}}} \mathop{\text{argmax}}_{\mathcal{F}_{disc}} [w_{Gan}\mathbf{L_{Gan}} + w_{rec}\mathbf{L_{rec}} + w_{local}\mathbf{L_{local}}]. \tag{8}$$

Subsequently, we train $\mathcal{F}_o$ and $\mathcal{F}_d$ to obtain the optimized semantic classifier keeping other parameters fixed.

$$\mathop{\arg\min}_{\mathcal{F}_o, \mathcal{F}_d} [\mathbf{L_{dom}} + \mathbf{L_{class}} + w_f\mathbf{L_{sem}}]. \tag{9}$$

**Algorithm 1** ODG-NET training algorithm

**Require:** Initialized $\mathcal{F}_G, \mathcal{F}_{im}, \mathcal{F}_v, \mathcal{F}_y, \mathcal{F}_\eta, \mathcal{F}_d, \mathcal{F}_o, \mathcal{F}_{disc}, \{\mathcal{F}_l^s\}_{l=1}^{\mathcal{S}}$

1: **while** Not Converged **do**

2: Sample a batch of $(x_r, y, v_d)$ from $\mathcal{D}$ and $\eta_1 \sim \mathcal{N}(0, \mathbb{I}), \eta_2 \sim \mathcal{N}(0, \sigma), \eta_3 \sim \mathcal{N}(0, \mathbb{I})$. $\sigma$ is the noise variance for generating the pseudo-open samples.

3: Generate $\hat{v}_d$s and $\hat{y}$s using Dirichlet($\alpha$). $\alpha$ is the parameter of the distribution.

4: Obtain a batch of $x_f^{cs} = \mathcal{F}_G(x_r, \hat{v}_d, y, \eta_1)$.

5: Obtain a batch of $x_f^{os} = \mathcal{F}_G(x_r, v_d/\hat{v}_d, \hat{y}, \eta_2)$.

6: Obtain $x_r^{rec} = \mathcal{F}_G(x_f^{cs/os}, v_d, y, \eta_3)$.

7: Obtain $Fe_l$, the latent representation corresponding to $(x_r, x_f^{os}, x_f^{cs}, x_r^{rec})$.

8: Obtain $Fe_d$, the attended domain features, and $Fe_o$, the attended semantic features from $Fe_l$.

9: Solve: $\mathop{\text{argmin}}_{\substack{\mathcal{F}_{im}, \mathcal{F}_v, \mathcal{F}_y, \mathcal{F}_\eta, \mathcal{F}_G, \\ \{\mathcal{F}_l^s\}_{s=1}^{\mathcal{S}}}} \mathop{\text{argmax}}_{\mathcal{F}_{disc}} [w_{Gan}\mathbf{L_{Gan}} + w_{rec}\mathbf{L_{rec}} + w_{local}\mathbf{L_{local}}]$.

10: Solve: $\mathop{\text{argmin}}_{\mathcal{F}_o, \mathcal{F}_d} [\mathbf{L_{dom}} + \mathbf{L_{class}} + w_f\mathbf{L_{sem}}]$.

11: **end while**

**Testing**. During inference, images from $\mathcal{D}_\mathcal{T}$ are provided as input to $\{\mathcal{F}_l^s\}_{s=1}^{\mathcal{S}}$. The class labels with the highest softmax probability scores are predicted according to $\mathcal{F}_o$.

## 4 Experimental Evaluations

**Datasets**. We present our results on six widely used benchmark datasets for DG. Specifically, we follow the approach of Shu et al. (2021) and use the following datasets: (1) **Office-Home** Venkateswara et al. (2017), (2) **PACS** Li et al.

Table 1: Comparative analysis for PACS and Office-Home on ODG. (In %)

| Methods | Art | | Sketch | | Photo | | Cartoon | | Avg | | Clipart | | Real-World | | Product | | Art | | Avg | |
|---|---|---|---|---|---|---|---|---|---|---|---|---|---|---|---|---|---|---|---|---|
| | Acc | H-score | Acc | H-score | Acc | H-score | Acc | H-score | Acc | H-score | Acc | H-score | Acc | H-score | Acc | H-score | Acc | H-score | Acc | H-score |
| AGG | 51.35 | 38.87 | 49.75 | 47.09 | 53.15 | 44.19 | 66.43 | 48.98 | 55.17 | 44.78 | 42.83 | 44.98 | 62.40 | 53.67 | 54.27 | 50.11 | 42.22 | 40.87 | 50.43 | 47.41 |
| MLDG Li et al. (2018a) | 44.59 | 31.54 | 51.29 | 49.91 | 62.20 | 43.35 | 71.64 | 55.20 | 57.43 | 45.00 | 41.82 | 41.26 | 62.98 | 55.84 | 56.89 | 52.25 | 42.58 | 40.97 | 51.07 | 47.58 |
| FC Li et al. (2019b) | 51.12 | 39.01 | 51.15 | 49.28 | 60.94 | 45.79 | 69.32 | 52.67 | 58.13 | 46.69 | 41.80 | 41.65 | 63.79 | 55.16 | 54.41 | 52.02 | 44.13 | 43.25 | 51.03 | 48.02 |
| Epi-FCR Li et al. (2019a) | 54.16 | 41.16 | 46.35 | 46.14 | 70.03 | 48.38 | 72.00 | 58.19 | 60.64 | 48.47 | 37.13 | 42.05 | 62.60 | 54.73 | 54.95 | 52.68 | 46.33 | 44.46 | 50.25 | 48.48 |
| PAR Wang et al. (2020b) | 52.97 | 39.21 | 53.62 | 52.00 | 51.86 | 36.53 | 67.77 | 52.05 | 56.56 | 44.95 | 41.27 | 41.77 | 65.98 | 57.60 | 55.37 | 54.13 | 42.40 | 42.62 | 51.26 | 49.03 |
| RSC Huang et al. (2020) | 50.47 | 38.43 | 50.17 | 44.59 | 67.53 | 49.82 | 67.51 | 47.35 | 58.92 | 45.05 | 38.60 | 38.39 | 60.85 | 53.73 | 54.61 | 54.66 | 44.19 | 44.77 | 49.56 | 47.89 |
| CuMix Mancini et al. (2020a) | 53.85 | 38.67 | 37.70 | 28.71 | 65.67 | 49.28 | 74.16 | 47.53 | 57.85 | 41.05 | 41.54 | 43.07 | 64.63 | 58.02 | 57.74 | 55.79 | 42.76 | 40.72 | 51.67 | 49.40 |
| Fish Shi et al. (2021) | 52.22 | 39.54 | 55.54 | 54.28 | 69.41 | 48.87 | 69.85 | 51.75 | 61.75 | 48.61 | 43.76 | 44.38 | 65.25 | 58.74 | 57.86 | 57.33 | 49.78 | 46.57 | 54.16 | 51.75 |
| Disentanglement Zhang et al. (2022) | 53.18 | 38.32 | 56.39 | 53.36 | 71.99 | 47.39 | 70.54 | 50.63 | 63.02 | 47.42 | 44.89 | 42.87 | 63.38 | 59.51 | 58.88 | 55.44 | 45.49 | 43.43 | 53.16 | 50.31 |
| Mixstyle Zhou et al. (2021) | 53.41 | 39.33 | 56.10 | 54.44 | 72.37 | 47.21 | 71.54 | 52.22 | 63.35 | 48.30 | 42.28 | 41.15 | 61.78 | 60.23 | 59.92 | 53.97 | 50.11 | 42.78 | 53.52 | 49.53 |
| DAML Shu et al. (2021) | 54.10 | 43.02 | 58.50 | 56.73 | 75.69 | 53.29 | 73.65 | 54.47 | 65.49 | 51.88 | 45.13 | 43.12 | 65.99 | 60.13 | 61.54 | 59.00 | 53.13 | 51.11 | 56.45 | 53.34 |
| DAML + OpenMax Bendale & Boult (2016a) | 52.73 | 41.28 | 57.81 | 56.82 | 74.55 | 54.55 | 75.84 | 55.96 | 65.23 | 52.15 | 45.51 | 44.25 | 60.33 | 61.46 | 60.71 | 59.67 | 51.34 | 52.34 | 54.47 | 54.43 |
| **ODG-NET** | **57.21** | **46.19** | **61.85** | **59.25** | **78.76** | **56.67** | **77.39** | **61.11** | **68.80** | **55.81** | **49.81** | **48.39** | **68.45** | **63.33** | **63.29** | **61.51** | **56.05** | **53.52** | **59.40** | **56.69** |

Table 2: Comparative analysis for VLCS and Digits-DG on ODG. (In %)

| Methods | Caltech | | LabelMe | | Pascal VOC | | Sun | | AVG | | MNIST | | MNIST_M | | SVHN | | SYN | | AVG | |
|---|---|---|---|---|---|---|---|---|---|---|---|---|---|---|---|---|---|---|---|---|
| | Acc | H-score | Acc | H-score | Acc | H-Score | Acc | H-score | Acc | H-score | Acc | H-score | Acc | H-score | Acc | H-Score | Acc | H-score | Acc | H-score |
| EPI-FCR Li et al. (2019a) | 66.81 | 62.98 | 47.83 | 45.33 | 50.22 | 45.56 | 46.03 | 44.32 | 52.72 | 49.55 | 72.39 | 68.33 | 45.83 | 43.34 | 51.27 | 46.88 | 62.46 | 60.23 | 57.98 | 54.69 |
| AGG | 65.49 | 62.59 | 46.15 | 42.78 | 48.29 | 44.31 | 44.48 | 40.67 | 51.10 | 47.58 | 69.45 | 63.28 | 43.51 | 42.15 | 50.26 | 46.89 | 61.87 | 56.31 | 56.27 | 52.15 |
| MLDG Li et al. (2018a) | 66.91 | 63.11 | 45.65 | 41.76 | 48.37 | 42.71 | 44.29 | 42.22 | 51.30 | 47.45 | 71.33 | 69.22 | 43.19 | 41.78 | 48.73 | 45.37 | 61.28 | 58.22 | 56.13 | 53.64 |
| PAR Wang et al. (2020b) | 65.78 | 61.25 | 46.21 | 42.54 | 50.11 | 46.33 | 45.39 | 43.65 | 51.87 | 48.44 | 70.88 | 67.47 | 44.62 | 42.65 | 49.34 | 45.72 | 60.23 | 57.11 | 56.26 | 53.23 |
| FC Li et al. (2019b) | 65.59 | 60.48 | 45.23 | 44.22 | 49.23 | 45.89 | 45.32 | 44.45 | 51.34 | 48.76 | 71.29 | 66.29 | 41.22 | 40.67 | 47.72 | 44.41 | 59.33 | 55.67 | 54.89 | 51.76 |
| RSC Huang et al. (2020) | 64.43 | 61.39 | 45.61 | 43.71 | 48.60 | 42.65 | 45.76 | 42.71 | 51.10 | 47.61 | 72.77 | 66.34 | 42.27 | 41.43 | 48.32 | 45.59 | 62.41 | 57.26 | 56.44 | 52.65 |
| CuMix Mancini et al. (2020a) | 66.21 | 63.76 | 46.72 | 45.59 | 50.54 | 45.78 | 46.38 | 45.33 | 52.46 | 50.11 | 72.10 | 67.52 | 45.88 | 43.74 | 52.22 | 47.22 | 62.33 | 58.33 | 58.13 | 54.20 |
| Fish Shi et al. (2021) | 65.82 | 62.29 | 47.66 | 46.52 | 50.11 | 45.53 | 45.54 | 43.33 | 52.28 | 49.41 | 74.43 | 66.89 | 42.65 | 44.45 | 52.31 | 46.71 | 64.76 | 58.73 | 58.53 | 54.19 |
| Disentanglement Zhang et al. (2022) | 63.27 | 61.86 | 48.65 | 45.39 | 50.53 | 43.22 | 46.72 | 45.76 | 52.29 | 49.05 | 71.29 | 68.83 | 45.38 | 41.59 | 50.16 | 42.71 | 65.66 | 60.33 | 58.12 | 53.36 |
| Mixstyle Zhou et al. (2021) | 66.11 | 63.19 | 46.72 | 46.22 | 49.75 | 46.19 | 46.62 | 46.87 | 52.30 | 50.61 | 76.56 | 70.56 | 47.81 | 45.66 | 54.97 | 47.24 | 61.80 | 61.96 | 60.23 | 56.35 |
| DAML Shu et al. (2021) | 69.18 | 64.65 | 48.22 | 47.71 | 49.87 | 47.22 | 46.87 | 46.78 | 53.53 | 51.59 | 73.98 | 69.88 | 46.49 | 45.62 | 53.34 | 47.72 | 64.22 | 59.23 | 59.51 | 55.61 |
| DAML + OpenMax Bendale & Boult (2016a) | 68.24 | 66.51 | 46.43 | 46.18 | 52.49 | 47.00 | 47.43 | 47.71 | 53.64 | 51.85 | 75.77 | 71.38 | 48.51 | 47.49 | 55.61 | 49.69 | 65.49 | 62.77 | 61.34 | 57.83 |
| **ODG-NET** | **73.42** | **69.93** | **51.89** | **51.56** | **53.44** | **52.75** | **50.21** | **50.14** | **57.24** | **56.09** | **78.56** | **75.75** | **50.52** | **50.22** | **57.81** | **52.62** | **68.94** | **65.33** | **63.85** | **60.98** |

(2017), (3) **Multi-Dataset** Shu et al. (2021). In addition, we introduce the experimental setup of ODG for two additional DG datasets, namely **VLCS** Fang et al. (2013) and **Digits-DG** Zhou et al. (2020b) in this paper. For our closed-set DG experiment, we also utilize the large-scale **DomainNet** Peng et al. (2019).

**Implementation details:** To ensure clarity, we use a ResNet-18 based backbone He et al. (2016) for $\mathcal{F}_o$ consistently, while we adopt standard architectures per benchmark for closed-DG tasks, following established literature Zhou et al. (2020b). Our attention modules $(\mathcal{A}_d, \mathcal{A}_o)$ are composed of a pair of spatial and spectral attention modules, implemented using the query-key-value processing-based approach Han et al. (2022). In total, ODG-NET comprises $48$ million parameters for $\mathcal{S} = 3$, and the training stage requires $65$ GFLOPS.

**Training protocol and model selection**. We employ a standardized training protocol across all datasets. During each training iteration, we first optimize Eq. 8 using the Adam optimizer Kingma & Ba (2014), with a learning rate of $2e-4$ and betas of $(0.5, 0.99)$. We then minimize Eq. 9 using Adam with a learning rate of $2e-2$ and betas of $(0.9, 0.99)$. Our batch size is typically set to $64$, and we train for $30$ epochs, except for DomainNet, where we use a batch size of $128$ and train for $40$ epochs. We follow a cross-validation approach, holding out $10\%$ of samples per domain and using held-out pseudo-open-set validation samples obtained through cumix Mancini et al. (2020b), that the model has not seen to select the best-performing model. In this regard, the mixup samples do not have a clear semantic meaning as they are generated by randomly combining two images. Hence, they can be considered representative open samples. We further consider $\beta = 0.5$ to put $\mathcal{W}$ as a soft constraint in $\mathbf{L_{GAN}}$. A large $\beta$ instigates the generation of ambiguous images in order to make them different from $\mathcal{D}$.

**Evaluation protocol**. For ODG experiments, we report the top-1 accuracy for closed-set samples (Acc) and the H-score for closed and open samples. For closed-set DG experiments, we consider the top-1 performance. We report the `mean` $\pm$ `std.` over three runs.

### 4.1 Results on open DG tasks

**Baselines**. Our baseline method, AGG, involves merging the source domains with different label sets and training a unified classifier on all the classes. In comparison, we evaluate the performance of ODG-NET against traditional DG methods that are less sensitive to label changes between different source domains, as outlined in Shu et al. (2021). These include state-of-the-art meta-learning-based and augmentation-based DG methods Li et al. (2018a; 2019a);

Table 3: Comparative analysis for Multi-Dataset on ODG. (In %)

| Methods | Clipart | | Real | | Painting | | Sketch | | Avg | |
|---|---|---|---|---|---|---|---|---|---|---|
| | Acc | H-score | Acc | H-score | Acc | H-Score | Acc | H-score | Acc | H-score |
| AGG | 29.78 | 34.06 | 65.33 | 64.72 | 44.30 | 51.04 | 27.59 | 35.41 | 41.75 | 46.31 |
| MLDG Li et al. (2018a) | 29.66 | 35.11 | 65.37 | 54.40 | 44.04 | 50.53 | 26.83 | 34.57 | 41.48 | 43.65 |
| FC Li et al. (2019b) | 29.91 | 35.42 | 64.77 | 63.65 | 44.13 | 50.07 | 28.56 | 34.10 | 41.84 | 45.81 |
| Epi-FCR Li et al. (2019a) | 27.70 | 37.62 | 60.31 | 64.95 | 39.57 | 50.24 | 26.76 | 33.74 | 38.59 | 46.64 |
| PAR Wang et al. (2020b) | 29.29 | 39.99 | 64.09 | 62.59 | 42.36 | 46.37 | 30.21 | 39.96 | 41.49 | 47.23 |
| RSC Huang et al. (2020) | 27.57 | 34.98 | 60.36 | 60.02 | 37.76 | 42.21 | 26.21 | 30.44 | 37.98 | 41.91 |
| CuMix Mancini et al. (2020a) | 30.03 | 40.18 | 64.61 | 65.07 | 44.37 | 48.70 | 29.72 | 33.70 | 42.18 | 46.91 |
| Fish Shi et al. (2021) | 32.78 | 35.42 | 65.43 | 67.77 | 45.37 | 48.81 | 32.35 | 32.45 | 43.98 | 46.11 |
| Disentanglement Zhang et al. (2022) | 28.76 | 33.33 | 64.48 | 64.44 | 42.29 | 50.05 | 30.65 | 35.87 | 41.54 | 45.92 |
| Mixstyle Zhou et al. (2021) | 30.03 | 40.18 | 64.61 | 65.07 | 44.37 | 48.70 | 29.72 | 33.70 | 42.18 | 46.91 |
| DAML Shu et al. (2021) | 37.62 | 44.27 | 66.54 | 67.80 | 47.80 | 52.93 | 34.48 | 41.82 | 46.61 | 51.71 |
| DAML Shu et al. (2021) + OpenMax Bendale & Boult (2016a) | 38.55 | 45.51 | 66.87 | 68.89 | 48.51 | 53.12 | 35.61 | 42.56 | 47.38 | 52.52 |
| **ODG-NET** | **40.75** | **47.54** | **69.49** | **71.22** | **50.11** | **55.39** | **37.58** | **44.10** | **49.48** | **54.56** |


Figure 3: (a) Depiction of the generated pseudo-open-set samples by ODG-NET. (b) Depiction of the pseudo-stylized images (columns 2-4) generated by ODG-NET concerning the input images mentioned in column 1. (c) Results of the intermediate images showing the transition between a pair of domain/label. We show two intermediate images for both cases.

Mancini et al. (2020a); Zhou et al. (2021); Shi et al. (2021); Rame et al. (2022), heterogeneous DG Li et al. (2019b), and methods that produce discriminative and generic embedding spaces Wang et al. (2020b); Huang et al. (2020); Zhang et al. (2022). As per Shu et al. (2021), we employ a confidence-based classifier for our competitors. Here, a sample is classified as unknown if the class probabilities are below a predefined threshold. Alternatively, we also compare against the only existing ODG technique, DAML Shu et al. (2021) and consider a variant where we combine DAML with Openmax Bendale & Boult (2016b) based OSR.

**Quantitative and qualitative analysis**. Tables 1-3 present a performance comparison of ODG-NET with the literature on five datasets. Our method consistently outperforms others in terms of Acc and H-score for all domain combinations and the average leave-one-out case where all the domains except one are used during training and the model is validated on the held-out target domain. For example, on PACS, ODG-NET achieves an Acc of $68.80\%$ and an H-score of $55.81\%$, surpassing the previous best of DAML+OpenMax which obtained $65.23\%$ and $52.15\%$, respectively. Our method outperforms Shu et al. (2021) by $\approx 3\%$ for Office-Home and $\approx 5\%$ for VLCS and Digits-DG in H-score. For the challenging and large-scale Multi-dataset, ODG-NET achieves an Acc of $49.48\%$ and an H-score of $54.56\%$, which is an improvement of more than $3\%$ than Shu et al. (2021). Visually, the T-SNE Van der Maaten & Hinton (2008) Fig. 4(a) confirms the discriminative and domain-independent nature of the semantic space given the augmented source data.

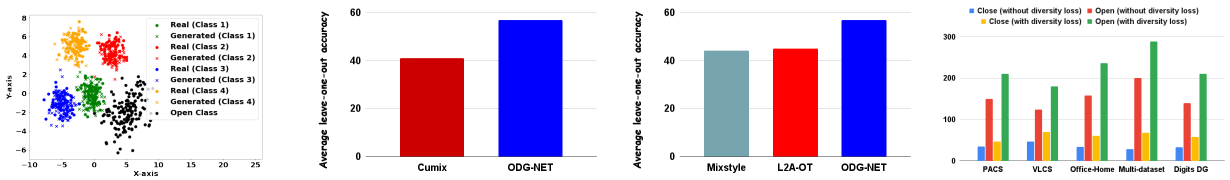


(a) (b) (c) (d)

Figure 4: (a) T-SNE of real and cGAN synthesized images in the semantic feature space $\mathcal{F}_o^b$ for PACS dataset. (b) Accuracy comparison between ODG-NET and Cumix Mancini et al. (2020a) based pseudo-open sample generation. (c) Accuracy comparison between ODG-NET and Mixstyle Zhou et al. (2021) and L2A-OT Zhou et al. (2020b) based closed-set sample generation. (d) The Frećhet distance Dowson & Landau (1982) between real data and the closed and pseudo-open images generated, with and without the consideration of $\mathcal{W}$ in $\mathbf{L_{Gan}}$.

Moreover, we present a collection of synthetically created images produced by our novel ODG-NET. As illustrated in Figure 3, (a) displays the generated pseudo-open-set examples, while (b) exhibits the pseudo-stylized pictures (columns 2-4) derived from their corresponding input images (column 1). This comparison highlights the evident transformation from the original input images to the synthesized pseudo images. Additionally, in (c), we demonstrate two aspects: first, the variation in artistic style of the input image, such as from sketch to painting; second, the combined shift in both style and label, exemplified by the transition from a "dog" class image to a "bag" class image.

Table 4: Results of PACS, VLCS, Office-Home, Digits-DG and DomainNet datasets under close-set DG. (In %)

| Methods | PACS | VLCS | Office-Home | Digits-DG | DomainNet |
|---|---|---|---|---|---|
| CCSA Motiian et al. (2017) | 79.40 | 70.20 | 64.90 | 74.50 | - |
| SFA-A Li et al. (2021c) | 81.70 | 74.00 | - | 79.60 | - |
| MetaReg Balaji et al. (2018) | 81.70 | - | - | - | 43.62 |
| MixStyle Zhou et al. (2021) | 83.70 | - | 65.50 | - | 34.0 |
| JiGen Carlucci et al. (2019) | 80.51 | 73.19 | 61.20 | 76.20 | - |
| SagNet Wu et al. (2019) | 83.25 | - | 62.34 | - | 40.30 |
| RSC Huang et al. (2020) | 85.15 | 75.43 | 63.12 | - | 38.90 |
| DDAIG Zhou et al. (2020a) | 83.10 | - | 65.50 | 77.58 | - |
| L2A-OT Zhou et al. (2020b) | 82.80 | - | 65.60 | 78.10 | - |
| FACT Xu et al. (2021) | 84.51 | - | 66.56 | 81.55 | - |
| STEAM Chen et al. (2021) | 86.60 | - | 66.80 | 83.13 | - |
| Style Neo. Kang et al. (2022) | 85.47 | - | 65.89 | - | 44.60 |
| Liu et al. Liu et al. (2021) | - | 76.48 | 67.85 | 80.02 | - |
| MMD-AAE Li et al. (2018b) | 77.00 | 72.30 | 62.70 | 74.60 | - |
| Cross-Grad Shankar et al. (2018) | 80.70 | - | 64.40 | 75.83 | - |
| MASF Dou et al. (2019) | 81.03 | 74.11 | - | - | - |
| EISNet Wang et al. (2020a) | 82.15 | 74.65 | - | - | - |
| MetaVIB Du et al. (2020) | - | 74.54 | - | - | - |
| DGER Zhao et al. (2020) | - | 74.38 | - | - | - |
| MixUp Zhang et al. (2017) | - | - | - | - | 39.20 |
| DMG Chattopadhyay et al. (2020) | - | - | - | - | 43.63 |
| SWAD Cha et al. (2021) | 88.10 | 79.10 | 70.60 | - | 46.50 |
| Fish Shi et al. (2021) | 85.50 | 77.80 | 68.60 | - | 42.70 |
| DAML Shu et al. (2021) | 82.70 | 72.95 | 67.71 | 79.89 | - |
| **ODG-NET** | **90.66** | **79.85** | **72.92** | **86.75** | **50.16** |

## 4.2 Results on closed DG tasks

In the context of closed-set DG tasks, we compare the performance of ODG-NET against the existing literature, focusing on supervised pre-training methods that use meta-learning, regularization, and domain augmentation techniques Zhou et al. (2020b; 2021); Chen et al. (2021); Kang et al. (2022); Chattopadhyay et al. (2020); Xu et al. (2021); Shu et al. (2021); Shi et al. (2021); Du et al. (2020); Zhao et al. (2020), among others.

As shown in Table 4 for the five benchmark DG datasets, ODG-NET outperforms all comparative techniques in the average leave-one-out DG evaluations, despite these techniques being designed explicitly for closed-set DG. We observe an improvement of at least $3-4\%$ across all datasets. For DomainNet, ODG-NET achieves an average accuracy of $50.16\%$, which is $4\%$ better than the previous state-of-the-art method SWAD Cha et al. (2021), likely due to the more diversified training set on which ODG-NET is trained. Finally, in closed-set DG experiments, ODG-NET outperforms DAML Shu et al. (2021) by a significant margin of at least $5-7\%$.

Table 5: Model and loss ablation analysis on PACS & Office-Home datasets. (In %)

| Model variants of ODG-NET | PACS | | Office-Home | |
|---|---|---|---|---|
| | Acc | H-score | Acc | H-score |
| **- w/o** ($\mathcal{F}_{im}, \mathcal{F}_v, \mathcal{F}_y, \mathcal{F}_\eta$) | 63.43 | 50.82 | 53.07 | 50.55 |
| **- w/o** $\mathcal{A}_d$ **and** $\mathcal{A}_o$ | 66.01 | 52.93 | 56.58 | 53.53 |
| **- w/o** $\{\mathcal{F}_l^s\}_{s=1}^S$**, but a common backbone for the source domains** | 63.73 | 51.53 | 53.14 | 50.50 |
| **- w/o** $\mathcal{F}_d$ | 64.98 | 52.09 | 55.55 | 52.69 |
| **- w/o** $\mathcal{F}_d$ **and** $\{\mathcal{F}_l^s\}_{s=1}^S$ | 62.38 | 49.67 | 51.95 | 49.02 |
| **- w/o Entropy loss** | 66.81 | 53.15 | 57.35 | 54.36 |
| **- w/o** $\mathbf{L_{con}}$ | 65.36 | 51.73 | 55.40 | 51.60 |
| **- w/o** $\mathbf{L_{sem}}$ | 64.74 | 51.12 | 54.57 | 51.11 |
| **- w/o** $\mathcal{F}_d$ **and** $\{\mathcal{F}_l^s\}_{s=1}^S$ **and** $\mathbf{L_{sem}}$ | 59.07 | 47.07 | 48.91 | 45.56 |
| **- with training** $\mathcal{F}_o$ **from scratch** | 65.96 | 52.86 | 56.38 | 53.33 |
| **- w/o** $\mathcal{W}$ **in** $\mathbf{L_{GAN}}$ | 66.26 | 53.96 | 58.38 | 54.93 |
| **Sensitivity to noise variance of GAN for synthesizing closed and pseudo-open samples** | | | | |
| $P_{noise}^{cs} - \mathcal{N}(0,1)$; $P_{noise}^{os} - \mathcal{N}(0,1)$ | 65.30 | 52.51 | 55.38 | 52.53 |
| $P_{noise}^{cs} - \mathcal{N}(0,1)$; $P_{noise}^{os} - \mathcal{N}(0,2)$ | 66.35 | 53.32 | 56.44 | 53.40 |
| $P_{noise}^{cs} - \mathcal{N}(0,1)$; $P_{noise}^{os} - \mathcal{N}(0,3)$ | 67.29 | 54.21 | 57.18 | 54.49 |
| $P_{noise}^{cs} - \mathcal{N}(0,1)$; $P_{noise}^{os} - \mathcal{N}(0,4)$ | 67.98 | 55.14 | 58.29 | 55.52 |
| $P_{noise}^{cs} - \mathcal{N}(0,1)$; $P_{noise}^{os} - \mathcal{N}(0,10)$ | 68.22 | 55.37 | 58.72 | 56.11 |
| $P_{noise}^{cs} - \mathcal{N}(0,5)$; $P_{noise}^{os} - \mathcal{N}(0,5)$ | 67.13 | 54.22 | 55.65 | 52.24 |
| **ODG-NET**($P_{noise}^{cs} - \mathcal{N}(0,1)$; $P_{noise}^{os} - \mathcal{N}(0,5)$) | **68.80** | **55.81** | **59.40** | **56.69** |

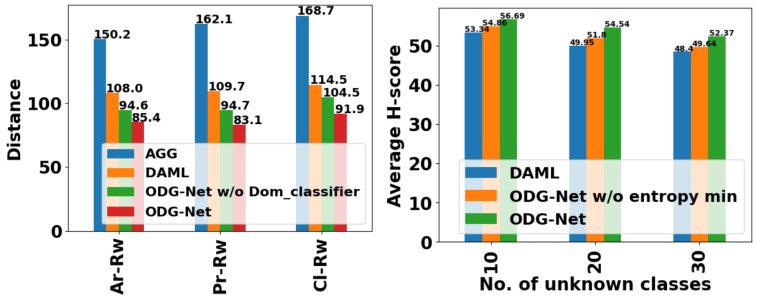


(a) (b)

Figure 5: (a) Frećhet distance between the source and target domains for the closed-set classes. (b) Openness analysis.

### 4.3 Ablation analysis

**Model and loss ablation**. In Table 5, we present the effects of different components of the ODG-NET model and the loss functions for PACS and Office-Home datasets. We confirmed that embedding networks are crucial for learning latent conditioning information in a meaningful way. The model without embedding layers resulted in a performance drop of approximately $5-6\%$ in the H-score. Similarly, attention modules helped to highlight the style and semantic features better, and using $(\mathcal{A}_d, \mathcal{A}_o)$ resulted in a $3-4\%$ improvement in the H-score for both datasets. Additionally, we experimented with using a common backbone for the source domains instead of $\{\mathcal{F}_l^s\}_{s=1}^S$. This approach significantly reduced the H-score by $4\%$ and $6\%$ for both datasets, indicating the importance of multi-view features learned by the domain-specific backbones.

Furthermore, $\mathcal{F}_d$ helped to discriminate the domain and semantic properties of $Fe_l(x)$, and the omission of $\mathcal{F}_d$ reduced performance by almost $5\%$. We also removed both $\mathcal{F}_d$ and the local classifiers $\{\mathcal{F}_l^s\}_{l=1}^S$ simultaneously, resulting in a performance drop of over $6\%$. When we trained $\mathcal{F}_o$ from scratch instead of using a pre-trained ResNet-18 backbone, we observed a performance drop of around $3\%$. The pre-trained ResNet-18 backbone is already rich in discriminative information, which helps our DG tasks. Concerning the loss function of feature optimization, it is evident that both the closed-set contrastive and open-space entropy regularizer assists in generating a more discriminative feature space. The model without any of these losses or the full $\mathbf{L_{sem}}$ led to performance degradation by approximately $4\%$. Finally, we removed the diversity regularization $\mathcal{W}$ in $\mathbf{L_{GAN}}$. Although, as per Fig. 4(d), $\mathcal{W}$ induces diversity in the generated images, empirically, we observed a nominal change in the accuracy $(1-1.5\%)$ in the presence of $\mathcal{W}$.

**Comparison of our augmentation with methods from the literature**. Our augmentation technique enables more controlled style and label mix-up, and we compared it against two types of augmentation techniques from the literature: existing style diversification approaches Zhou et al. (2020b; 2021) for closed-set classes, and Cumix Mancini et al. (2020a), which performs random image mix-up so that the generated images can be a proxy for open-space. Our results in Fig. 4(b)-4(c) demonstrate that ODG-NET performs better with our proposed augmentation. Our method is interpolation-based, which allows us to generate more style primitives than Zhou et al. (2020b). Since our method is image-based as opposed to the feature-based method of Zhou et al. (2021), we can handle the semantics better. Similarly, for pseudo-open samples, we can generate more meaningful images with varied similarities to the closed classes than the random mix-up of Mancini et al. (2020a).

**Sensitivity to variances of $P_{noise}^{os/cs}$**. In this experiment, we tune the $\sigma$ parameter of $P_{noise}^{os}$ while fixing $P_{noise}^{cs}$ for $\mathcal{F}_G$. As shown in Table 5, we observe that as we increase $\sigma$ from 1 to 5, the model performance continuously improves from $52.51\%$ to $55.81\%$ for PACS and from $52.53\%$ to $56.69\%$ for Office-Home. With high variance, the open samples are sparsely distributed, better covering the open space. However, the performance improvements are found to saturate beyond $\sigma = 5$. On the other hand, increasing the variance of $P_{noise}^{cs}$ significantly affects the performance, leading to a drop of at least $3\%$. This occurs because the generated images may deviate from the original semantic concepts, degrading the quality of the generated images.

**Frećhet distance for domain alignment**. To assess the domain independence of $\mathcal{F}_o^b$, we calculate the Frećhet distance Dowson & Landau (1982) between the closed-set classes of the source and target domains for Office-Home, with the target domain being *Real-world*. In Fig. 5(a), we show the Frećhet distance of the baseline AGG, DAML, and two variants of ODG-NET, with and without the domain classifier $\mathcal{F}_d$. The full ODG-NET produces the minimum Frećhet distance, indicating that it performs the best domain alignment among the compared models. The model without $\mathcal{F}_d$ performs poorly compared to the full ODG-NET, suggesting that the use of $\mathcal{F}_d$ helps disentangle features better, making $\mathcal{F}_o^b$ less affected by domain properties and focus on shared components.

**Sensitivity to number of target open classes**. Since there is no restriction on the number of open classes in the target domain, we are interested in assessing whether ODG-NET can handle different numbers of open classes during inference. Here, we considered the average leave-one-out H-score for Office-Home and simulated three scenarios with different numbers of open classes in the target: 10, 20, and 30. As shown in Figure 5(b), ODG-NET consistently outperforms DAML Shu et al. (2021) by at least $3\%$ for different openness factors. The entropy minimization component of $\mathbf{L_{sem}}$ widens the gap between open and closed spaces, which is helpful in this regard. We validate this by removing the entropy component of $\mathbf{L_{sem}}$ and re-running the experiments, in which case we find that performance drops by $2 - 3\%$.

**Performance comparison when the source domains have a disjoint set of classes.** Here, we present a novel experimental scenario in ODG, where the source domains have completely different sets of classes, and the target domain consists of all the classes from the sources, plus previously unknown class samples. We compare the performance of ODG-NET with that of DAML Shu et al. (2021) for this setup in Table 6. We find that ODG-NET outperforms DAML by around $3\%$, demonstrating its robustness to extreme domain and label shifts within the source domains.

Table 6: Comparison between DAML Shu et al. (2021) and ODG-NET when the source domains have mutually disjoint classes on Office-Home dataset in terms of H-score. (In $\%$)

| Domain | Clipart | RealWorld | Product | Art | Average |
|---|---|---|---|---|---|
| DAMLShu et al. (2021) | 40.12 | 58.72 | 54.85 | 47.25 | 50.23 |
| ODG-NET | 45.69 | 62.77 | 56.95 | 49.86 | 53.81 |

## 5 Takeaways

In this paper, we present ODG-NET, a solution to the challenging problem of open domain generalization. This task combines domain generalization, open-set learning, and class imbalance in a common setting. One of the key features of ODG-NET is the novel generative augmentation, which enables continuous domain and label conditional image synthesis through interpolation of conditioning variables. This augmented training set is utilized to learn a discriminative and unbiased semantic space for an open-set classifier while minimizing the effects of domain-dependent artifacts. In our experiments, ODG-NET achieves state-of-the-art performance for both open-set and closed-set domain generalization on six benchmark datasets. We plan to extend our evaluation to more safety-critical applications in the future.

## References


Yogesh Balaji, Swami Sankaranarayanan, and Rama Chellappa. Metareg: Towards domain generalization using meta-regularization. *Advances in neural information processing systems*, 31, 2018.

Abhijit Bendale and Terrance E Boult. Towards open set deep networks. In *Proceedings of the IEEE conference on computer vision and pattern recognition*, pp. 1563–1572, 2016a.

Abhijit Bendale and Terrance E Boult. Towards open set deep networks. In *Proceedings of the IEEE conference on computer vision and pattern recognition*, pp. 1563–1572, 2016b.

Ruichu Cai, Zijian Li, Pengfei Wei, Jie Qiao, Kun Zhang, and Zhifeng Hao. Learning disentangled semantic representation for domain adaptation. In *IJCAI: proceedings of the conference*, volume 2019, pp. 2060. NIH Public Access, 2019.

Fabio M Carlucci, Antonio D'Innocente, Silvia Bucci, Barbara Caputo, and Tatiana Tommasi. Domain generalization by solving jigsaw puzzles. In *Proceedings of the IEEE/CVF Conference on Computer Vision and Pattern Recognition*, pp. 2229–2238, 2019.

Junbum Cha, Sanghyuk Chun, Kyungjae Lee, Han-Cheol Cho, Seunghyun Park, Yunsung Lee, and Sungrae Park. Swad: Domain generalization by seeking flat minima. *Advances in Neural Information Processing Systems*, 34: 22405–22418, 2021.

Prithvijit Chattopadhyay, Yogesh Balaji, and Judy Hoffman. Learning to balance specificity and invariance for in and out of domain generalization. In *European Conference on Computer Vision*, pp. 301–318. Springer, 2020.

Yang Chen, Yu Wang, Yingwei Pan, Ting Yao, Xinmei Tian, and Tao Mei. A style and semantic memory mechanism for domain generalization. In *Proceedings of the IEEE/CVF International Conference on Computer Vision*, pp. 9164–9173, 2021.

Andrea Dittadi, Frederik Träuble, Francesco Locatello, Manuel Wüthrich, Vaibhav Agrawal, Ole Winther, Stefan Bauer, and Bernhard Schölkopf. On the transfer of disentangled representations in realistic settings. *arXiv preprint arXiv:2010.14407*, 2020.

Qi Dou, Daniel Coelho de Castro, Konstantinos Kamnitsas, and Ben Glocker. Domain generalization via model-agnostic learning of semantic features. *Advances in Neural Information Processing Systems*, 32, 2019.

DC Dowson and BV666017 Landau. The fréchet distance between multivariate normal distributions. *Journal of multivariate analysis*, 12(3):450–455, 1982.

Yingjun Du, Jun Xu, Huan Xiong, Qiang Qiu, Xiantong Zhen, Cees GM Snoek, and Ling Shao. Learning to learn with variational information bottleneck for domain generalization. In *European Conference on Computer Vision*, pp. 200–216. Springer, 2020.

Chen Fang, Ye Xu, and Daniel N. Rockmore. Unbiased metric learning: On the utilization of multiple datasets and web images for softening bias. In *Proceedings of the IEEE International Conference on Computer Vision (ICCV)*, December 2013.

Rui Gong, Wen Li, Yuhua Chen, and Luc Van Gool. Dlow: Domain flow for adaptation and generalization. In *Proceedings of the IEEE/CVF conference on computer vision and pattern recognition*, pp. 2477–2486, 2019.

Ian Goodfellow, Jean Pouget-Abadie, Mehdi Mirza, Bing Xu, David Warde-Farley, Sherjil Ozair, Aaron Courville, and Yoshua Bengio. Generative adversarial networks. *Communications of the ACM*, 63(11):139–144, 2020.

Kai Han, Yunhe Wang, Hanting Chen, Xinghao Chen, Jianyuan Guo, Zhenhua Liu, Yehui Tang, An Xiao, Chunjing Xu, Yixing Xu, et al. A survey on vision transformer. *IEEE transactions on pattern analysis and machine intelligence*, 2022.

Kaiming He, Xiangyu Zhang, Shaoqing Ren, and Jian Sun. Deep residual learning for image recognition. In *Proceedings of the IEEE conference on computer vision and pattern recognition*, pp. 770–778, 2016.

Zeyi Huang, Haohan Wang, Eric P Xing, and Dong Huang. Self-challenging improves cross-domain generalization. In *European Conference on Computer Vision*, pp. 124–140. Springer, 2020.

Juwon Kang, Sohyun Lee, Namyup Kim, and Suha Kwak. Style neophile: Constantly seeking novel styles for domain generalization. In *Proceedings of the IEEE/CVF Conference on Computer Vision and Pattern Recognition*, pp. 7130–7140, 2022.

Diederik P Kingma and Jimmy Ba. Adam: A method for stochastic optimization. *arXiv preprint arXiv:1412.6980*, 2014.

Diederik P Kingma and Max Welling. Auto-encoding variational bayes. *arXiv preprint arXiv:1312.6114*, 2013.

Da Li, Yongxin Yang, Yi-Zhe Song, and Timothy M Hospedales. Deeper, broader and artier domain generalization. In *Proceedings of the IEEE international conference on computer vision*, pp. 5542–5550, 2017.

Da Li, Yongxin Yang, Yi-Zhe Song, and Timothy Hospedales. Learning to generalize: Meta-learning for domain generalization. In *Proceedings of the AAAI conference on artificial intelligence*, volume 32, 2018a.

Da Li, Jianshu Zhang, Yongxin Yang, Cong Liu, Yi-Zhe Song, and Timothy M Hospedales. Episodic training for domain generalization. In *Proceedings of the IEEE/CVF International Conference on Computer Vision*, pp. 1446–1455, 2019a.

Haoliang Li, Sinno Jialin Pan, Shiqi Wang, and Alex C Kot. Domain generalization with adversarial feature learning. In *Proceedings of the IEEE conference on computer vision and pattern recognition*, pp. 5400–5409, 2018b.

Haoliang Li, YuFei Wang, Renjie Wan, Shiqi Wang, Tie-Qiang Li, and Alex Kot. Domain generalization for medical imaging classification with linear-dependency regularization. *Advances in Neural Information Processing Systems*, 33:3118–3129, 2020.

Jingjing Li, Erpeng Chen, Zhengming Ding, Lei Zhu, Ke Lu, and Heng Tao Shen. Maximum density divergence for domain adaptation. *IEEE Transactions on Pattern Analysis and Machine Intelligence*, 43(11):3918–3930, 2021a. doi: 10.1109/TPAMI.2020.2991050.

Lei Li, Ke Gao, Juan Cao, Ziyao Huang, Yepeng Weng, Xiaoyue Mi, Zhengze Yu, Xiaoya Li, and Boyang Xia. Progressive domain expansion network for single domain generalization. In *Proceedings of the IEEE/CVF Conference on Computer Vision and Pattern Recognition*, pp. 224–233, 2021b.

Pan Li, Da Li, Wei Li, Shaogang Gong, Yanwei Fu, and Timothy M Hospedales. A simple feature augmentation for domain generalization. In *Proceedings of the IEEE/CVF International Conference on Computer Vision*, pp. 8886–8895, 2021c.

Yiying Li, Yongxin Yang, Wei Zhou, and Timothy Hospedales. Feature-critic networks for heterogeneous domain generalization. In *International Conference on Machine Learning*, pp. 3915–3924. PMLR, 2019b.

Chang Liu, Lichen Wang, Kai Li, and Yun Fu. *Domain Generalization via Feature Variation Decorrelation*, pp. 1683–1691. Association for Computing Machinery, New York, NY, USA, 2021. ISBN 9781450386517. URL https://doi.org/10.1145/3474085.3475311.

Massimiliano Mancini, Zeynep Akata, Elisa Ricci, and Barbara Caputo. Towards recognizing unseen categories in unseen domains. In *European Conference on Computer Vision*, pp. 466–483. Springer, 2020a.

Massimiliano Mancini, Zeynep Akata, Elisa Ricci, and Barbara Caputo. Towards recognizing unseen categories in unseen domains. In *European Conference on Computer Vision*, pp. 466–483. Springer, 2020b.

Saeid Motiian, Marco Piccirilli, Donald A Adjeroh, and Gianfranco Doretto. Unified deep supervised domain adaptation and generalization. In *Proceedings of the IEEE international conference on computer vision*, pp. 5715–5725, 2017.

Cheng Ouyang, Chen Chen, Surui Li, Zeju Li, Chen Qin, Wenjia Bai, and Daniel Rueckert. Causality-inspired single-source domain generalization for medical image segmentation. *arXiv preprint arXiv:2111.12525*, 2021.

Novi Patricia and Barbara Caputo. Learning to learn, from transfer learning to domain adaptation: A unifying perspective. In *Proceedings of the IEEE Conference on Computer Vision and Pattern Recognition*, pp. 1442–1449, 2014.

Xingchao Peng, Qinxun Bai, Xide Xia, Zijun Huang, Kate Saenko, and Bo Wang. Moment matching for multi-source domain adaptation. In *Proceedings of the IEEE/CVF international conference on computer vision*, pp. 1406–1415, 2019.

Mohammad Mahfujur Rahman, Clinton Fookes, Mahsa Baktashmotlagh, and Sridha Sridharan. Multi-component image translation for deep domain generalization. In *2019 IEEE Winter Conference on Applications of Computer Vision (WACV)*, pp. 579–588. IEEE, 2019.

Alexandre Rame, Corentin Dancette, and Matthieu Cord. Fishr: Invariant gradient variances for out-of-distribution generalization. In *International Conference on Machine Learning*, pp. 18347–18377. PMLR, 2022.

Shiv Shankar, Vihari Piratla, Soumen Chakrabarti, Siddhartha Chaudhuri, Preethi Jyothi, and Sunita Sarawagi. Generalizing across domains via cross-gradient training. *arXiv preprint arXiv:1804.10745*, 2018.

Yuge Shi, Jeffrey Seely, Philip HS Torr, N Siddharth, Awni Hannun, Nicolas Usunier, and Gabriel Synnaeve. Gradient matching for domain generalization. *arXiv preprint arXiv:2104.09937*, 2021.

Yang Shu, Zhangjie Cao, Chenyu Wang, Jianmin Wang, and Mingsheng Long. Open domain generalization with domain-augmented meta-learning. In *Proceedings of the IEEE/CVF Conference on Computer Vision and Pattern Recognition*, pp. 9624–9633, 2021.

Laurens Van der Maaten and Geoffrey Hinton. Visualizing data using t-sne. *Journal of machine learning research*, 9 (11), 2008.

Hemanth Venkateswara, Jose Eusebio, Shayok Chakraborty, and Sethuraman Panchanathan. Deep hashing network for unsupervised domain adaptation. In *Proceedings of the IEEE conference on computer vision and pattern recognition*, pp. 5018–5027, 2017.

Jingye Wang, Ruoyi Du, Dongliang Chang, Kongming Liang, and Zhanyu Ma. Domain generalization via frequency-domain-based feature disentanglement and interaction. In *Proceedings of the 30th ACM International Conference on Multimedia*, pp. 4821–4829, 2022.

Shujun Wang, Lequan Yu, Caizi Li, Chi-Wing Fu, and Pheng-Ann Heng. Learning from extrinsic and intrinsic supervisions for domain generalization. In *European Conference on Computer Vision*, pp. 159–176. Springer, 2020a.

Yufei Wang, Haoliang Li, and Alex C Kot. Heterogeneous domain generalization via domain mixup. In *ICASSP 2020-2020 IEEE International Conference on Acoustics, Speech and Signal Processing (ICASSP)*, pp. 3622–3626. IEEE, 2020b.

Ziqi Wang, Marco Loog, and Jan van Gemert. Respecting domain relations: Hypothesis invariance for domain generalization. In *2020 25th International Conference on Pattern Recognition (ICPR)*, pp. 9756–9763. IEEE, 2021.

Zhijie Wu, Xiang Wang, Di Lin, Dani Lischinski, Daniel Cohen-Or, and Hui Huang. Sagnet: Structure-aware generative network for 3d-shape modeling. *ACM Transactions on Graphics (TOG)*, 38(4):1–14, 2019.

Qinwei Xu, Ruipeng Zhang, Ya Zhang, Yanfeng Wang, and Qi Tian. A fourier-based framework for domain generalization. In *Proceedings of the IEEE/CVF Conference on Computer Vision and Pattern Recognition*, pp. 14383–14392, 2021.

Zheng Xu, Wen Li, Li Niu, and Dong Xu. Exploiting low-rank structure from latent domains for domain generalization. In *European Conference on Computer Vision*, pp. 628–643. Springer, 2014.

Shiqi Yang, Yaxing Wang, Kai Wang, Shangling Jui, and Joost van de Weijer. One ring to bring them all: Towards open-set recognition under domain shift. *arXiv preprint arXiv:2206.03600*, 2022.

Sangdoo Yun, Dongyoon Han, Seong Joon Oh, Sanghyuk Chun, Junsuk Choe, and Youngjoon Yoo. Cutmix: Regularization strategy to train strong classifiers with localizable features. In *Proceedings of the IEEE/CVF international conference on computer vision*, pp. 6023–6032, 2019.

Hanlin Zhang, Yi-Fan Zhang, Weiyang Liu, Adrian Weller, Bernhard Schölkopf, and Eric P Xing. Towards principled disentanglement for domain generalization. In *Proceedings of the IEEE/CVF Conference on Computer Vision and Pattern Recognition*, pp. 8024–8034, 2022.

Hongyi Zhang, Moustapha Cisse, Yann N Dauphin, and David Lopez-Paz. mixup: Beyond empirical risk minimization. *arXiv preprint arXiv:1710.09412*, 2017.

Chao Zhao and Weiming Shen. Adaptive open set domain generalization network: Learning to diagnose unknown faults under unknown working conditions. *Reliability Engineering & System Safety*, 226:108672, 2022.

Shanshan Zhao, Mingming Gong, Tongliang Liu, Huan Fu, and Dacheng Tao. Domain generalization via entropy regularization. *Advances in Neural Information Processing Systems*, 33:16096–16107, 2020.

Kaiyang Zhou, Yongxin Yang, Timothy Hospedales, and Tao Xiang. Deep domain-adversarial image generation for domain generalisation. In *Proceedings of the AAAI Conference on Artificial Intelligence*, volume 34, pp. 13025–13032, 2020a.

Kaiyang Zhou, Yongxin Yang, Timothy Hospedales, and Tao Xiang. Learning to generate novel domains for domain generalization. In *European conference on computer vision*, pp. 561–578. Springer, 2020b.

Kaiyang Zhou, Yongxin Yang, Yu Qiao, and Tao Xiang. Domain generalization with mixstyle. *arXiv preprint arXiv:2104.02008*, 2021.

Kaiyang Zhou, Ziwei Liu, Yu Qiao, Tao Xiang, and Chen Change Loy. Domain generalization: A survey. *IEEE Transactions on Pattern Analysis and Machine Intelligence*, 2022.

Ronghang Zhu and Sheng Li. Crossmatch: Cross-classifier consistency regularization for open-set single domain generalization. In *International Conference on Learning Representations*, 2021.